Development 138, 2717-2727 (2011) doi:10.1242/dev.059030

Alk3 controls nephron number and androgen production via lineage-specific effects in intermediate mesoderm

Valeria Di Giovanni[1,2], Adrian Alday[1], Lijun Chi[1], Yuji Mishina[3] and Norman D. Rosenblum[1,2,4,*]

SUMMARY

The mammalian kidney and male reproductive system are both derived from the intermediate mesoderm. The spatial and temporal expression of bone morphogenetic protein (BMP) 2 and BMP4 and their cognate receptor, activin like kinase 3 (ALK3), suggests a functional role for BMP-ALK3 signaling during formation of intermediate mesoderm-derivative organs. Here, we define cell autonomous functions for *Alk3* in the kidney and male gonad in mice with CRE-mediated *Alk3* inactivation targeted to intermediate mesoderm progenitors (*Alk3*$^{IMP\ null}$). *Alk3*-deficient mice exhibit simple renal hypoplasia characterized by decreases in both kidney size and nephron number but normal tissue architecture. These defects are preceded by a decreased contribution of *Alk3*-deleted cells to the metanephric blastema and reduced expression of *Osr1* and SIX2, which mark nephron progenitor cells. Mutant mice are also characterized by defects in intermediate mesoderm-derived genital tissues with fewer mesonephric tubules and testicular Leydig cells, epithelial vacuolization in the postnatal corpus epididymis, and decreased serum testosterone levels and reduced fertility. Analysis of ALK3-dependent signaling effectors revealed lineage-specific reduction of phospho-p38 MAPK in metanephric mesenchyme and phospho-SMAD1/5/8 in the testis. Together, these results demonstrate a requirement for *Alk3* in distinct progenitor cell populations derived from the intermediate mesoderm.

KEY WORDS: *Alk3*, Intermediate Mesoderm, Nephron, Mouse

INTRODUCTION

The intermediate mesoderm gives rise to two distinct organ systems within the urogenital tract: the metanephric kidneys, and the gonads and their associated duct structures (Saxen, 1987; Joseph et al., 2009). The intermediate mesoderm is specified, in part, by bone morphogenetic proteins (Dressler, 2009; Preger-Ben Noon et al., 2009). After gastrulation, a renal progenitor cell population, marked by expression of odd-skipped-related (*Osr*) 1, arises from the intermediate mesoderm along an anterior-posterior axis. The demonstration that overexpression of a constitutive active activin-like-kinase (ALK) 3 receptor in the chick intermediate mesoderm generates dose-dependent regulation of *Osr1* expression (James and Schultheiss, 2005) suggested a functional role for ALK3. However, the function of endogenous BMP signaling during specification of the intermediate mesoderm is undefined.

Murine urogenital development commences at embryonic day (E) 8.0 with the formation of intermediate mesoderm-derived paired epithelial tubes, the nephric ducts, in the urogenital ridge bilateral to the midline. Initially, a transient kidney-like structure, the pronephros, is induced by the nephric duct only to degenerate completely (Saxen et al., 1986; Saxen and Sariola, 1987; Kuure et al., 2000). Coincident with their caudal migration at E9.5, the nephric ducts each induce formation of the mesonephric tubules from the intermediate mesoderm (Kuure et al., 2000). Ultimately, mesonephric cells only contribute to the testis. By E10.5, a caudal region of the nephric duct forms an epithelial outgrowth termed the ureteric bud in response to signals from the intermediate mesoderm-derived metanephric blastema. Permanent metanephric kidney development commences with invasion of the blastema by the ureteric bud.

Kidney organogenesis is dependent on reciprocal signaling between the ureteric bud and what is now the metanephric mesenchyme (Grobstein, 1956; Saxen and Sariola, 1987). A subset of cells in the metanephric mesenchyme express *Osr1*, which is required for the differentiation of the derivative renal stromal and nephrogenic lineages (Mugford et al., 2008). Metanephric mesenchyme-derived signals trigger elongation and repetitive branching of the ureteric bud to form the collecting system. In turn, ureteric-derived signals induce aggregation of mesenchymal nephrogenic progenitor cells around ureteric bud tips. Nephrogenic cells either replenish the progenitor pool or undergo a mesenchyme-to-epithelial transition and form a succession of intermediate structures culminating in formation of the mature nephron (Vainio and Lin, 2002). The number of nephrons formed during nephrogenesis is an important determinant of human health. Reduced nephron endowment results in pathological states ranging from childhood renal failure to adult-onset hypertension, depending on the severity of nephron deficiency (Schedl, 2007; Cain et al., 2010).

Male genital tissues arise from intermediate mesoderm-derived mesonephric and nephric duct cells. The nephric duct contributes to formation of the epididymis and seminal vesicle (Dyche, 1979; Joseph et al., 2009). Mesonephric cells contribute to testicular androgen-producing Leydig cells and peritubular myoid cells (Buehr et al., 1993; Merchant-Larios et al., 1993). Formation of testicular seminiferous cords is dependent on migration of mesonephric endothelial cells (Combes et al., 2009). By contrast,

[1]Program in Developmental and Stem Cell Biology, Hospital for Sick Children, Toronto, ON M5G 1X8, Canada. [2]Department of Laboratory Medicine and Pathobiology, University of Toronto, Toronto, ON M5S 1A8, Canada. [3]Department of Biologic and Materials Science, School of Dentistry, University of Michigan, Ann Arbor, MI 48109-1078, USA. [4]Division of Nephrology, Department of Paediatrics, University of Toronto, Toronto, ON M5G 1X8, Canada.

*Author for correspondence (norman.rosenblum@sickkids.ca)

Accepted 13 April 2011

testicular Sertoli and germ cells are derived from coelomic epithelium and the epiblast, respectively (Lawson and Hage, 1994; Karl and Capel, 1998). The molecular mechanisms that control specification of intermediate mesoderm-derived progenitor cell populations into testicular cell populations are undefined.

BMPs bind to heteromeric complexes composed of type I (confers ligand specificity) and type II serine-threonine kinase receptors. The mode of ligand binding to the receptor complex dictates activation of distinct signaling effectors. BMP ligand, binding to pre-formed receptor complexes, activates phosphorylation of cytoplasmic SMAD 1/5/8 proteins (ten Dijke et al., 1994), while de novo formation of ligand-receptor complexes activates MAPKs, including p38 and ERK (Nohe et al., 2004). BMP2 and BMP4 are expressed as early as E7.5 in the intermediate mesoderm. *Bmp4*$^{-/-}$ mice die during gastrulation from defective posterior mesoderm formation (Winnier et al., 1995; Zhang and Bradley, 1996). Although analysis of deficient mice demonstrates that both *Bmp2* and *Bmp4* control primordial germ cell number, embryonic lethality in these and *Alk3*-deficient mice before other types of testicular cells are specified, has limited a more complete analysis of BMP function during testis development (Lawson et al., 1999; Ying and Zhao, 2001). The demonstration that knockdown of BMP expression results in defective pronephric formation in zebrafish combined with *Alk3* expression in the murine metanephric mesenchyme suggests a possible role for BMP signaling in murine nephrogenesis (Kishimoto et al., 1997; Dick et al., 2000).

Here, we investigated the functions of BMP-ALK3 signaling in mice in which *Alk3* deficiency is targeted to intermediate mesoderm progenitors and renal and genital derivatives. Our results demonstrate cell-autonomous functions for *Alk3* in the metanephric blastema and the testis. Renal embryogenesis in mutants is characterized by decreased participation of *Alk3*-deficient cells in formation of the metanephric blastema and derivative nephrons, resulting in a decrease in the nephrogenic progenitor cell population and simple renal hypoplasia. In addition, targeted *Alk3* deficiency results in perturbed formation of intermediate mesoderm-derived testicular cells and the corpus epididymis and decreased fertility. Analysis of ALK3-dependent signaling effectors revealed a lineage-specific reduction of phospho-p38 MAPK and phospho-SMAD1/5/8 in the metanephric mesenchyme and testis, respectively.

MATERIALS AND METHODS

Generation of mice model

Alk3$^{+/-}$ (CD1:C57BL/6) and *Rarb2*-Cre mice (CD1) (kindly provided by Cathy Mendelsohn, Columbia University, New York, USA) were intercrossed. *Rarb2*-Cre; *Alk3*$^{flox/-}$ mice were generated using *Rarb2*-Cre; *Alk3*$^{+/-}$ and *Alk3*$^{flox/flox}$ (C57BL6) mice. Mice were maintained on a mixed genetic background and genotyped by PCR (Mishina et al., 2002). *Alk3* heterozygotes (*Alk3*$^{+/-}$, *Rarb2*-Cre; *Alk3*$^{flox/+}$) were phenotypically identical to *Alk3* wild type (*Alk3*$^{flox/+}$) and both were used as controls. ROSA26-Cre reporter mice (*R26R*) were purchased from Jackson Laboratories (stock number 003310). Male gender was determined by PCR for the SRY locus (Lambert et al., 2000). Mice were housed in the Laboratory Animal Services facility, Hospital for Sick Children, Toronto. The presence of a copulatory plug in the morning was considered as E0.5.

β-Galactosidase staining

Frozen sections were fixed at 37°C for 15 minutes in *lacZ* fix (25% gluteraldehyde, 100 nM EGTA, 1 M $MgCl_2$, 0.1 sodium phosphate) and then incubated in *lacZ* stain (25 mg/ml X-gal, potassium ferrocyanide, potassium ferricyanide) solution at 37°C overnight in the dark. Embryos were fixed in *lacZ* fix, washed in wash (0.1 M sodium phosphate buffer, 2% nonidet-P40) solution and incubated in *lacZ* stain at 37°C overnight.

Immunohistochemistry, immunofluorescence and immunoblotting

Kidney, testes and seminal vesicles were fixed in 10% buffered formalin at RT and paraffin embedded. Nephron number was estimated by counting glomeruli in three tissue sections (4 μm) extending from the renal cortex through the papilla for each genotype. Cross-sectional area was measured by AxioVision 4.6.3-SP1 (Zeiss) software.

Immunohistochemisty was performed using 4 μm sections washed in xylene and re-hydrated in ethanol. Sections were sequentially treated with 3% H_2O_2, heated in a pressure cooker in 0.1 M sodium citrate/citric acid buffer (pH 6.0), blocked in a 30% BSA/goat serum solution and incubated with primary antibodies overnight at 4°C. Sections were incubated with anti-rabbit secondary (Vectastain, Vector Labs), followed by ABC (Vector Labs) and visualized by AEC (Zymed). Primary antibodies: anti-P-SMAD1/5/8 (1:150, Cell Signaling), anti-phospho-ERK1/2 (1:250, Cell Signaling) and anti-phospho-p38 MAPK (1:150, Cell Signaling).

For immunofluorescent microscopy, 4 μm sections were heated in a pressure cooker in 0.1 M sodium citrate buffer (pH 6.0). Sections were blocked as above and incubated with primary overnight at 4°C. Tissue was incubated with either Alexa 488/568 goat-anti-mouse/anti-rabbit secondary antibody (1:500, Molecular Probes) and DAPI for 1 hour at room temperature, mounted in VectaShield (Vector) and visualized on an AxioVert 200M (Zeiss) microscope. Primary antibodies: anti-CITED1 (1:200, NeoMarkers), anti-CYTOCHROME P450 (1:200, Abcam), anti-INSL3 (1:200, Phoenix Pharmaceuticals), anti-NCAM (1:150, Sigma), anti-PAX2 (1:200, Covance), anti-SALL1 (1:200, Abcam), anti-SIX2 (1:500, Proteintech), anti-SMA (1:250, Sigma) and anti-WT1 (1:1000, Santa Cruz).

For immunoblotting, 30 E13.5 kidneys were harvested per genotype. Primary antibodies: phospho-SMAD1/5/8 and total SMAD1 (1:250, Cell Signaling), and total p-38 MAPK (1:150, Cell Signaling).

In situ hybridization

Embryonic tissue was harvested at E12.5 and fixed in 4% PFA. Tissue was paraffin-embedded and sectioned (4 μm). RNA in situ hybridization was performed as described (Hartwig et al., 2008). Probe hybridization was visualized by BM Purple AP substrate (Roche). An *Alk3* exon 2-specific probe was used to assess *Alk3* deletion (Hebert et al., 2002).

In vitro culture conditions

E12.5 kidneys were cultured on 0.4 μm pore transfilter membranes (Becton Dickinson) in DMEM-F12 (Gibco) and apo-transferrin (Sigma) for 24 hours at 37°C in a CO_2 incubator. E11.5 urogenital ridges were cultured in the same manner for 4 hours. Tissue was fixed in methanol at –20°C and treated with 0.1% Triton-X 100. Tissue was blocked with 30% BSA and goat serum, and incubated with primary antibodies for 1 hour at 37°C. Primary antibodies: anti-CALBINDIN-D_{28k} (1:200, Sigma), anti-WT1 (1:100, Sigma) and anti-PAX2 (1:100, Covance). Explants were incubated with Alexa 488 goat anti-rabbit/Alexa 568 goat anti-mouse secondary antibody for 1 hour at 37°C and visualized on an AxioVert 200M (Zeiss) microscope.

Cell proliferation and apoptosis assays

Renal cell proliferation at E12.5 was assessed by incorporation of 5-bromo-2′ deoxyuridine (BrdU, Roche). Pregnant mice were administered BrdU via the peritoneum (100 mg/g of body weight) 2 hours prior to sacrifice. Tissue was processed as described (Cain et al., 2009). Apoptosis was assayed in E11.5 urogenital ridges and E12.5 kidneys using terminal deoxynucleotidyl transferase (TdT)-mediated dUTP Nick End Labeling (TUNEL) on paraffin sections following the manufacturer's instructions (Promega). In E10.5 and E11.5 embryos, apoptosis and proliferation were assessed by anti-activated caspase 3 (1:250, Cell Signaling) and anti-Ki67 (1:150, Dako), respectively. E11.5 mesonephric tubule proliferation was assessed by anti-PCNA antibody (1:500, Cell Signaling).

Serum testosterone assay

Total blood was collected by cardiac puncture from P30 male mice. Blood was separated into serum and submitted for serum testosterone analysis by tritium-based radioimmunoassay (IDEXX Labs).

Statistical analysis

Statistical analysis of nephron number and kidney area was performed by one-way ANOVA (GraphPad Prism, Version 5.0c). Kidney area was determined by measuring the outline of sagittal sections generated through the kidney midline using Image J software (n=3). Statistical analysis of apoptosis, proliferation, ureteric bud branch tips, Leydig cells and testosterone levels was performed using Student's t-test (Excel). The number of Leydig cells at E18.5 were quantitated by counting INSL3-positive cells in four randomly selected fields (three testis per genotype). At P30, Leydig cells were quantitated by counting CYTOCHROME P450-positive cells in 10 randomly selected fields, in three nonadjacent sections per testis, three animals per group, as previously reported (Hu et al., 2010).

RESULTS

Genetic model of *Alk3* deficiency in the intermediate mesoderm

Alk3 is expressed as early as E9.5 in the mesonephric epithelium and mesenchyme, the metanephric kidney and the gonad (Dewulf et al., 1995; Mishina et al., 1995; Hartwig et al., 2008). As homozygous *Alk3* deficiency results in lethality before the onset of urogenital development, *Alk3* function during formation of intermediate mesoderm-derived tissues is undefined (Mishina et al., 1995). Therefore, we generated mice with conditional inactivation of *Alk3* in intermediate mesoderm progenitors ($Alk3^{IMP\ null}$) using an $Alk3^{loxP}$ allele and Cre recombinase directed by the retinoic acid receptor β isoform 2 (*Rarb2)* promoter (Fig. 1A-F). The spatial domain of Cre recombinase expression under control of the *Rarb2* promoter was identified using the ROSA26 (*R26R*) reporter strain (Soriano, 1999). Consistent with a previous report (Kobayashi et al., 2005), *lacZ* expression marked the region of intermediate mesoderm that forms the metanephric blastema (Fig. 1A; see Fig. S1A in the supplementary material) and which contributes to renal mesenchyme cell aggregates, developing epithelial nephrogenic structures and nephrogenic tubules in *Rarb2*-Cre;*Rosa26* (*R26R*) embryos (Fig. 1B,C). *lacZ* expression was also observed in mesonephric tubules (Fig. 1D) and mesonephric-derived peritubular myoid and interstitial cells (Fig. 1E), but not in testicular endothelial, Sertoli or germ cells (Fig. 1E). Furthermore, *lacZ* marked the intermediate mesoderm-derived epididymis and mesonephric-derived interstitial cells between testicular seminiferous cords (Fig. 1E,F). Consistent with this pattern of expression, in $Alk3^{IMP\ null}$ mice, *Alk3* mRNA expression was not detected in uninduced metanephric mesenchyme cells, but was maintained in the ureteric bud (compare Fig. 1G with 1H), and was absent in mesonephric epithelium but was unaltered in the bi-potential gonad, prior to invasion by mesonephric cells (compare Fig. 1I with 1J). Thus, *Rarb2-Cre* targets *Alk3* deletion to intermediate mesoderm-derived nephrogenic precursors in the metanephric blastema and the epididymis, and in the mesonephros and derivative myoid and interstitial cells.

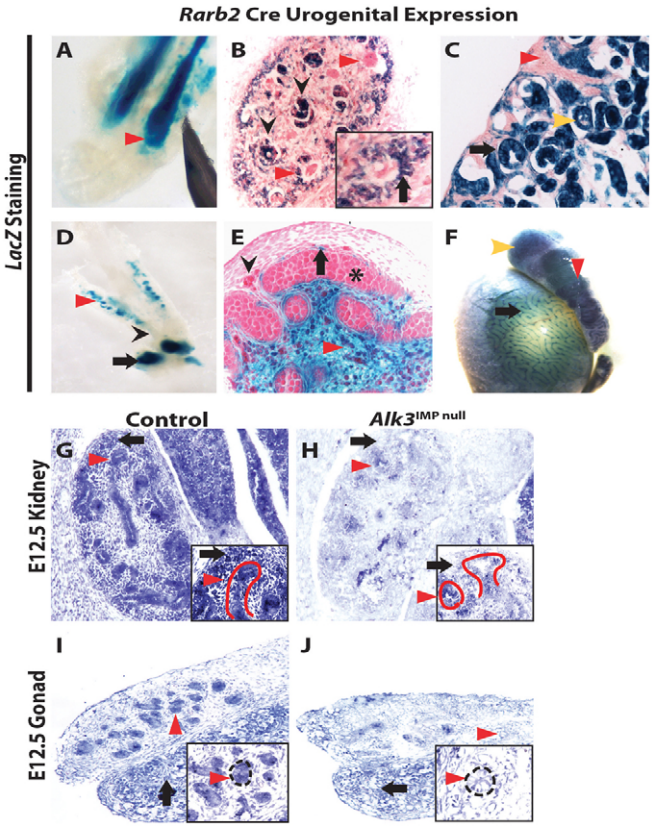

Fig. 1. Targeted deletion of *Alk3* to intermediate mesoderm progenitors. (A-F) *lacZ* expression as a marker of *Rarb2*-Cre activity. (**A**) Expression of *lacZ* in the E10.5 metanephric blastema (arrowhead). (**B**) At E12.5, *lacZ* was expressed in mesenchyme aggregates (arrow, inset) and developing nephrons (black arrowheads), but was absent from ureteric cells (red arrowhead). (**C**) At P4, all nephrogenic structures expressed *lacZ,* including tubules (arrow) and podocytes (yellow arrowhead). *lacZ* was not expressed in collecting ducts (red arrowheads). (**D**) In E11.5 urogenital ridges, *lacZ* marked the metanephric blastema (arrow) and mesonephros (red arrowhead), but not the in nephric duct (black arrowhead). (**E**) At E15.5, *lacZ* marked interstitial (red arrowhead) and peritubular myoid (arrow), but not endothelial (black arrowhead) and germ cells (asterisk). (**F**) At P30, *lacZ* was noted in interstitial cells (arrow), ductus epididymis (yellow arrowhead) and the epididymis (red arrowhead). (**G**) At E12.5, *Alk3* mRNA (blue) was observed in control ureteric cells (red arrowhead, red line, inset) and the metanephric mesenchyme (arrow). (**H**) In $Alk3^{IMP\ null}$ mice, *Alk3* mRNA was not detected in metanephric mesenchyme cells (arrow), but was present in ureteric cells (red arrowhead; red line, inset). (**I**,**J**) At E12.5, *Alk3* mRNA was expressed in gonads (arrow) and mesonephric tubules (arrowheads, inset) of controls (I), but was markedly reduced in mesonephric tubules (outline) of $Alk3^{IMP\ null}$ mice (arrowhead, inset) (J).

Alk3 deficiency in intermediate mesoderm progenitors results in renal hypoplasia

$Alk3^{IMP\ null}$ mice were recovered in the expected Mendelian ratio (152/698 recovered pups, 22%). The requirement for *Alk3* during kidney development was assessed by analyzing renal structure at P30, a stage after completion of nephrogenesis. Although renal architecture was normal, fewer glomeruli were observed in mutants, suggesting a defect in nephrogenesis (compare Fig. 2B with 2A). However, as 23% (5/22) of $Alk3^{IMP\ null}$ mice died in the perinatal period, it was possible that the P30 data were not indicative of the entire spectrum of mutants. Therefore, subsequent analyses were performed at E18.5, prior to the demise of mutants (Fig. 2C-I). At E18.5, renal histoarchitecture appeared normal but kidney area was reduced by 39% in $Alk3^{IMP\ null}$ mice compared with wild type and by 35% compared with $Alk3^{+/-}$ littermates (Fig. 2C-E). As embryo size was equivalent among wild-type, $Alk3^{+/-}$ and $Alk3^{IMP\ null}$ mice, the decrease in kidney area was not due to a generalized decrease in somatic growth (data not shown). Quantification of nephrons, identified by WT-1 expression, revealed a significant decrease in $Alk3^{IMP\ null}$ but not $Alk3^{+/-}$ mice

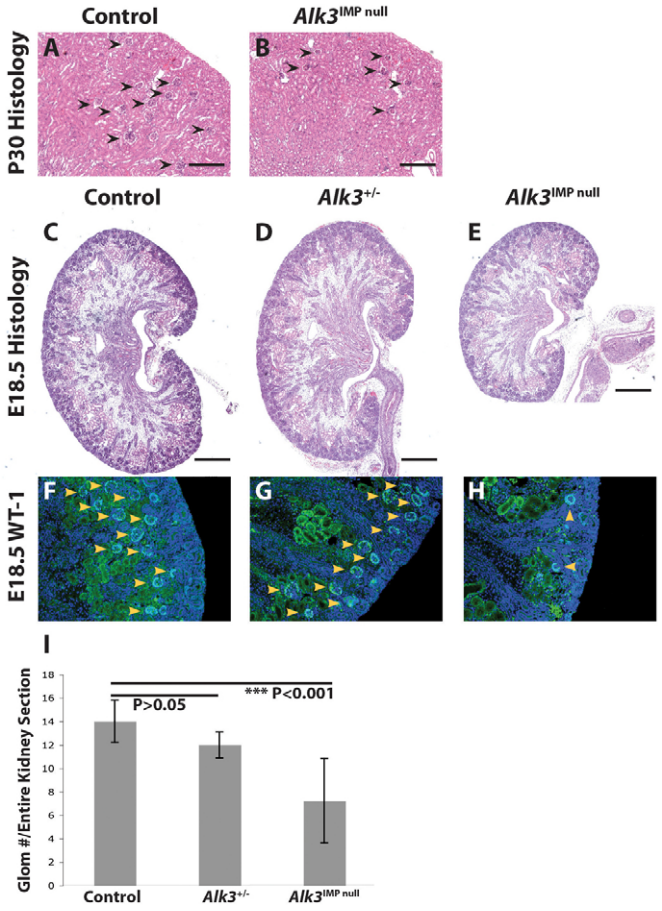

Fig. 2. Renal hypoplasia in *Alk3*$^{IMP\ null}$ mice. (**A**,**B**) P30 renal histology. The number of glomeruli (arrowhead) was greater in control (A) versus *Alk3*$^{IMP\ null}$ mice (B). Scale bars: 100 μm. (**C-E**) Cross-sectional area in wild type (C) and E18.5 *Alk3*$^{+/-}$ (D) mice was comparable and larger than in *Alk3*$^{IMP\ null}$ mice (E). Scale bars: 200 μm. (**F-I**) Glomerular number. Glomeruli were identified with anti-WT1 antibodies (arrowheads). Glomerular number in wild-type (F) and *Alk3*$^{+/-}$ (G) mice was comparable and greater than in *Alk3*$^{IMP\ null}$ mice (H). (I) *Alk3*$^{IMP\ null}$ WT1-positive glomeruli were significantly reduced in number (***P<0.001). Data are mean±s.e.m.

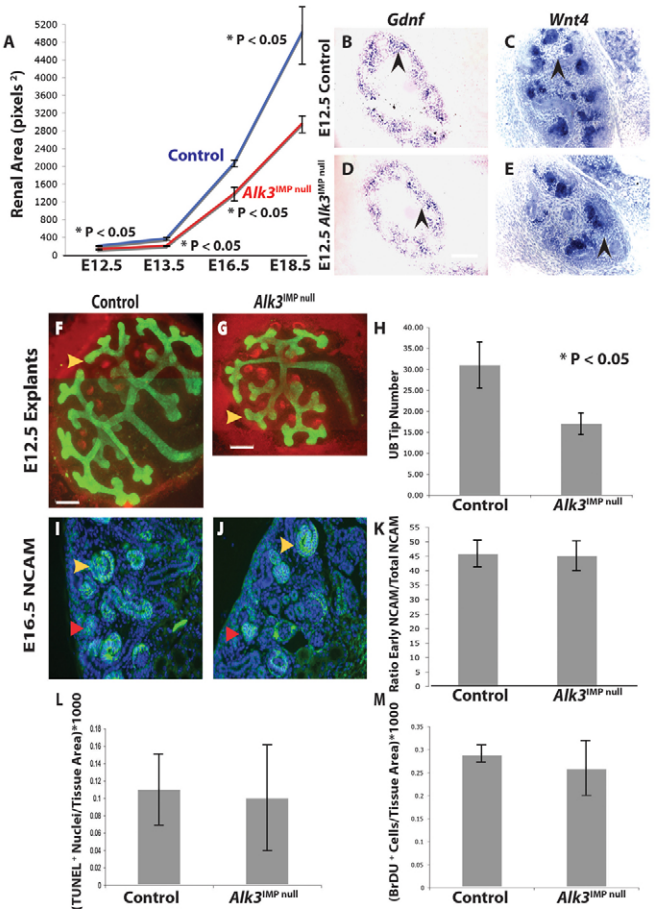

Fig. 3. Metanephric mesenchyme differentiation and survival is normal in *Alk3*$^{IMP\ null}$ kidneys. (**A**) Mutant kidney area was significantly reduced throughout embryogenesis (*P<0.05). Data are mean±s.e.m. (**B**,**D**) At E12.5, *Gdnf* (arrowheads) was expressed to a similar degree in the mesenchyme of control (B) and *Alk3*$^{IMP\ null}$ (D) kidneys. (**C**,**E**) *Wnt4* is expressed in renal aggregates (arrowheads) in both E12.5 control (C) and *Alk3*$^{IMP\ null}$ (E) kidneys. (**F**,**G**) Calbindin D_{28k} (green stain, yellow arrowhead) expression marked E12.5 ureteric bud tips in control (F) and *Alk3*$^{IMP\ null}$ (G) explants. WT1 expression (red) marked glomeruli. Scale bar: 200 pixels. (**H**) *Alk3*$^{IMP\ null}$ ureteric tip number was significantly reduced (*P<0.05). Data are mean±s.e.m. (**I**,**J**) NCAM marked early stage renal aggregates (red arrowheads) and advanced comma/S-shaped bodies (yellow arrowhead) in E16.5 control (I) and *Alk3*$^{IMP\ null}$ (J) sections. (**K-M**) The ratio of early stage versus total number of NCAM-positive nephrogenic precursor structures (K) and the rate of E12.5 apoptosis (L) and proliferation (M) were not significantly different in mutants versus controls (P>0.05). Data are mean±s.e.m.

(*P<0.001, Fig. 2H,I). Thus, *Alk3* deficiency in the metanephric mesenchyme causes simple renal hypoplasia defined as decreased kidney size and nephron number but normal tissue patterning.

Analysis of renal area in *Alk3*$^{IMP\ null}$ mice at progressively early stages of embryogenesis revealed that renal size was persistently decreased in mutants starting at E12.5 (Fig. 3A). Next, we analyzed the expression of genes required for nephrogenesis. *Gdnf* is expressed in the metanephric mesenchyme and signals via a GDNF-RET-WNT11 regulatory loop to control ureteric branching. Ureteric bud tips induce nephron formation, thereby controlling nephron number (Dziarmaga et al., 2003; Narlis et al., 2007). In *Alk3*$^{IMP\ null}$ mice, the expression of *Gdnf* was similar to that in controls (Fig. 3B,D). Despite this, the number of ureteric branch tips in E12.5 whole-mount kidney preparations were significantly decreased in *Alk3*$^{IMP\ null}$ mice (Fig. 3F-H). Yet, we could detect no decrease in the expression of *Ret* and *Wnt11* mRNA in mutants (see Fig. S1E,F,H,I in the supplementary material). Similarly, ureteric expression of *Wnt9b*, which is required for initiation of nephrogenesis (Carroll et al., 2005), was not disrupted in *Alk3*$^{IMP\ null}$ tissue (see Fig. S1G,J in the supplementary material). *Wnt4* is required for formation of nephrogenic aggregates and vesicles (Stark et al., 1994). Although we observed fewer *Wnt4*-positive nephrogenic structures in *Alk3*$^{IMP\ null}$ tissue, all intermediate nephrogenic structures present expressed *Wnt4* (Fig. 3C,E). Together, these data demonstrate decreased formation of nephrogenic precursor structures and associated ureteric branches in *Alk3*$^{IMP\ null}$ mice but no change in the expression of genes that control nephrogenesis and branching morphogenesis.

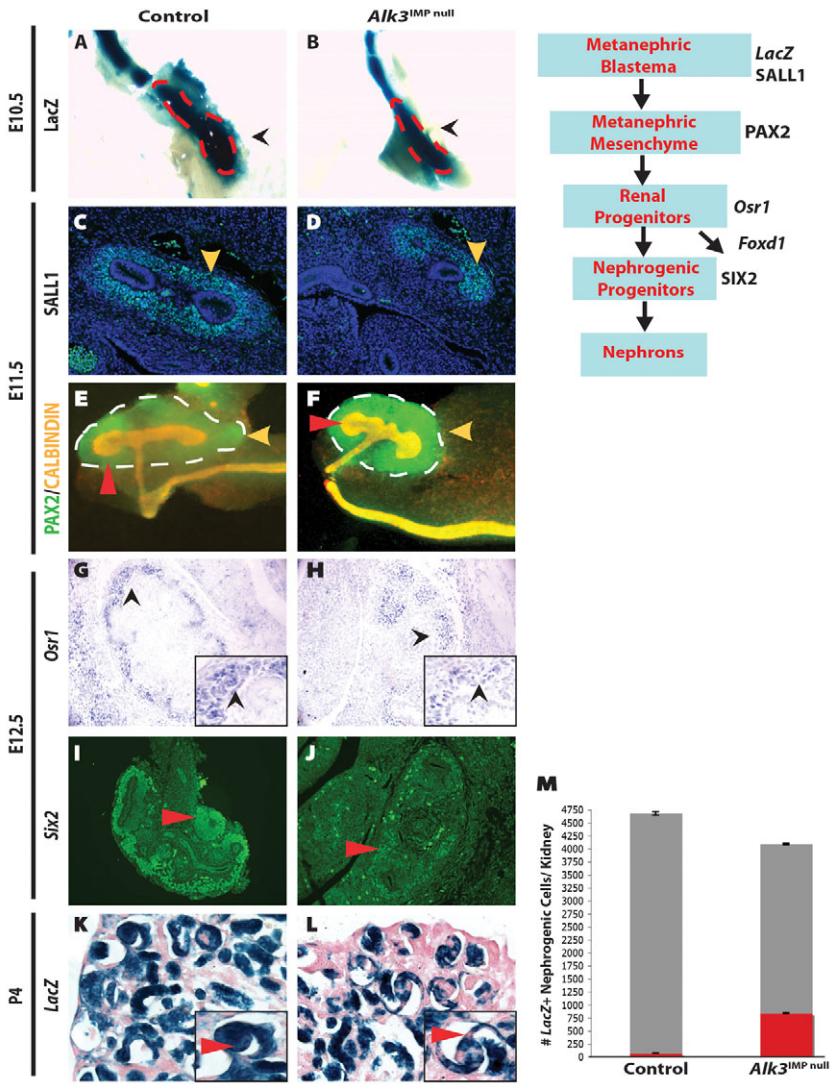

Fig. 4. Nephrogenic progenitor cells are decreased in *Alk3*$^{IMP\ null}$ animals. (**A**,**B**) The *lacZ*-positive (red outline) metanephric blastema (arrowheads) was larger in control (A) versus *Alk3*$^{IMP\ null}$ (B) (control mean=216 831 pixels^2, s.e.m.=15325; mutant mean=160 281 pixels^2, s.e.m.=34940). (**C**,**D**) The population of SALL1-expressing metanephric blastema cells (arrowheads) was larger in control (C) compared with mutants (D). (**F**) The E11.5 PAX2-positive metanephric mesenchyme (green stain, outline) around the initial ureteric bud (red arrowheads) was reduced in mutant animals (control mean=68907 pixels^2, s.e.m.=9950 pixels; mutant mean=30321 pixels^2, s.e.m.=3049 pixels). Yellow arrowheads indicate the metanephric mesenchyme. (**G-J**) Expression of the progenitor markers *Osr1* and SIX2 were reduced in *Alk3*$^{IMP\ null}$ kidneys (arrowheads, inset). (**K**,**L**) Pink indicates *lacZ*-negative cells (arrowhead, inset) incorporated into some P4 *Alk3*$^{IMP\ null}$ nephrogenic elements (L) compared with ubiquitous *lacZ* expression (arrowhead) in control nephrogenic elements (K). (**M**) At P4, nephrogenic cells were counted (six sections per kidney, three kidneys). *lacZ*-negative cells (red bar) accounted for 25% of all nephrogenic cells in mutants but only 1% in controls. Data are mean±s.e.m. Flow diagram depicts the sequence of specification of metanephric blastemal progenitor cell populations into the nephron lineage and molecular markers of specific specified cell populations.

We investigated the possibility that the deficit in nephrons in *Alk3*$^{IMP\ null}$ mice was due to defective progression of nephrogenic intermediates to mature nephrons. NCAM expression was used to mark nephrogenic intermediate structures at advancing stages of development, including pre-tubular aggregates and later nephrogenic structures (Klein et al., 1988). The ratio of immature nephrogenic structures (renal aggregates, vesicles) to total NCAM-expressing structures (including more mature comma and S-shaped bodies, renal tubules) was assessed at E16.5. Although a shift in this ratio towards more immature nephrogenic structures would reflect a delay in maturation in mutants, we observed no significant difference between *Alk3*$^{IMP\ null}$ and controls (Fig. 3I-K).

Next, we determined whether *Alk3*-dependent effects on nephrogenesis were associated with altered cell proliferation and/or apoptosis. First, we analyzed these events at the stage at which nephrogenesis is initiated (E12.5). Apoptotic nuclei were identified by TUNEL assay and proliferating cells were marked by BrdU incorporation (see Fig. S2A-D in the supplementary material). Quantification of the proportion of apoptotic and proliferating cells revealed no significant difference between controls and mutants (Fig. 3L,M). The expression of *Rarb2*-Cre in the intermediate mesoderm and metanephric blastema prior to the onset of renal development (Fig. 1A; see Fig. S1A in the supplementary material) suggested that a defect in intermediate mesoderm cell survival prior to nephrogenesis could cause early nephrogenic defects. Accordingly, we analyzed apoptosis and cell proliferation at a stage prior to the onset of nephrogenesis (E10.5, E11.5). At these early stages, the metanephric blastema in control and mutants was identified by expression of PAX2 (see Fig. S3A,D,G,J in the supplementary material). Proliferating and apoptotic cells were marked by Ki67 and anti-activated caspase 3, respectively (see Fig. S3A-K in the supplementary material). Quantification of apoptotic and proliferating cells as a fraction of the total number of metanephric blastema cells demonstrated no significant effect of *Alk3* deficiency (see Fig. S3C,F,I,L in the supplementary material).

Alk3 acts cell autonomously to control renal progenitor gene expression

Next, we investigated the contribution of *Alk3* to the population of nephrogenic precursors. Following formation of the metanephric blastema, mesenchyme cells, marked by the expression of specific genes, become progressively committed to a nephrogenic fate. Using these cell markers, we investigated whether *Alk3* deficiency negatively impacted the capacity to generate nephrogenic precursors (Fig. 4, schematic). We used the *R26R* allele in combination with *Rarb2-Cre* to mark the cells that constitute the

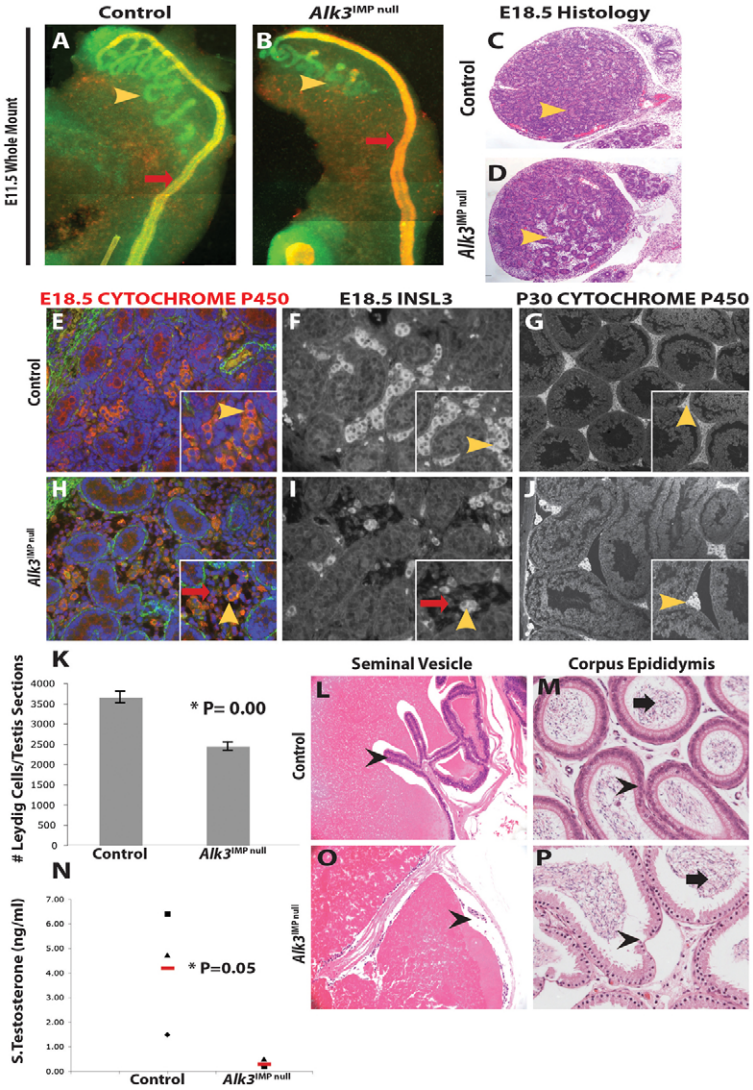

Fig. 5. Mesonephric-derived testicular cells are reduced in *Alk3*$^{IMP\ null}$ males. (**A**,**B**) In E11.5 whole-mount male urogenital ridges, calbindin D_{28K} expression marked nephric ducts (red arrows), whereas PAX2 expression (yellow arrowheads) marked the mesonephric tubules in control (A) and *Alk3*$^{IMP\ null}$ (B) mice. *Alk3*$^{IMP\ null}$ mice had significantly fewer tubules (*P<0.05, s.e.m.=0.58 (control) and 0.33 (mutant). (**C**,**D**) E18.5 testis histology. Fewer interstitial Leydig cells (arrowheads) were noted in mutant (D) versus control (C) testes. (**E**,**H**) Anti-cytochrome P450 expression identified Leydig cells. At E18.5, controls (E) contained more Leydig cells (yellow arrowheads) versus *Alk3*$^{IMP\ null}$ males (H). Mutants also contained undifferentiated interstitial cells (inset, arrow). SMA expression (green) marked peritubular myoid cells. (**F**,**I**) INSL3 expression also marked E18.5 Leydig cells. Controls (F) consisted of significantly more INSL3-positive cells (yellow arrowheads,*P=0.01, four sections per testis, three testis per genotype) compared with mutants (I). Red arrow indicates non INSL-expressing cells. (**G**,**J**) Mutants also contained undifferentiated cells (inset, arrow). At P30, a larger number of Leydig cells (arrowhead) were observed in controls (G) versus mutant (J) testes. (**K**) The number of mutant Leydig cells was significantly reduced (*P<0.001). Data are mean±s.e.m. (**L**,**O**) Seminal vesicle histology in 1-year old males. In *Alk3*$^{IMP\ null}$ males (O), the epithelial layer was thin and disorganized (arrowheads) compared with controls (L). (**M**,**P**) Corpus epididymis histology in 1-year old males. The epithelial cells in *Alk3*$^{IMP\ null}$ mice (P) demonstrated vacuolation (arrowheads) compared with the organized layer in controls (M). The mutant epididymis still contained sperm (arrows). (**N**) At P30, the average mean amount of serum testosterone (red bar) in *Alk3*$^{IMP\ null}$ males was significantly decreased (*P=0.05). Data are mean±s.e.m.

metanephric blastema prior to induction by the ureteric bud. At E10.5, *lacZ* expression demonstrated that the metanephric blastema was 56% smaller in *Alk3*$^{IMP\ null}$ embryos compared with controls (Fig. 4A,B). Consistent with this finding, the number of cells expressing SALL1, which marks blastemal mesenchyme cells, was markedly decreased in mutants at E11.5 (Fig. 4D). Similarly at E11.5, the size of the metanephric mesenchyme, demarcated by PAX2 expression, was 26% smaller in *Alk3*$^{IMP\ null}$ mice (Fig. 4E,F). Prior to the onset of nephrogenesis, *Osr1* is expressed in nephrogenic and stromal cell precursor cells (Mugford et al., 2008). At E12.5, expression of *Osr1* was reduced in *Alk3*$^{IMP\ null}$ mice (Fig. 4G,H). After E11.5, *Osr1*-expressing cells contribute to SIX2 expressing nephrogenic progenitors (Kobayashi et al., 2008; Mugford et al., 2008). SIX2 is required for maintenance of the self-renewing nephrogenic progenitor population (Self et al., 2006). In *Alk3*$^{IMP\ null}$ mice, SIX2 expression was reduced (Fig. 4J). CITED1 is expressed in non-self renewing SIX2-positive cells undergoing nephrogenesis. At E12.5, the number of CITED1-positive cells was significantly reduced in mutants (see Fig. S4C-E in the supplementary material).

Reduced SIX2 expression suggested that the nephrogenic progenitor pool could be prematurely exhausted in *Alk3*$^{IMP\ null}$ mice. At P4, an assessment of nephrogenic progenitor contribution to nephrogenesis was performed using the R26R allele and examining cortical sections for *lacZ* expression. *lacZ* marked cells contributed to 99% (4547 of 4613 cells) of nephrogenic structures in controls compared with only 75% (2413 of 3251 cells) in mutants (Fig. 4K-M). These results suggested that *Alk3*-deficient nephrogenic progenitors were depleted in *Alk3*$^{IMP\ null}$ mice resulting in integration of pink, *Rarb2*-Cre negative cells during nephrogenesis. The *Rarb2*-Cre negative cells may represent: (1) a mosaic expression of *Rarb2*-Cre in mesenchymal aggregates (Fig. 1B) and (2) in the context of *Alk3* deletion, a selective advantage for integration of *Rarb2*-Cre negative cells during nephrogenesis. *Osr1*-expressing cells also contribute to the renal stroma, which is marked by *Foxd1* expression. The *Foxd1* domain was also reduced in mutants (see Fig. S4B in the supplementary material), further demonstrating that *Alk3* regulates *Osr1*-positive renal progenitor cells.

Alk3 signaling controls mesonephric tubule number and mesonephros-derived testicular cells

The expression of *Rarb2*-Cre in progenitor mesonephric tubules (Fig. 1D) provided a basis to investigate the requirement for *Alk3* in specification of testicular cells of intermediate mesoderm origin. *Alk3* mRNA expression was reduced in *Alk3*$^{IMP\ null}$ mesonephric tubules, which were decreased in number compared with controls

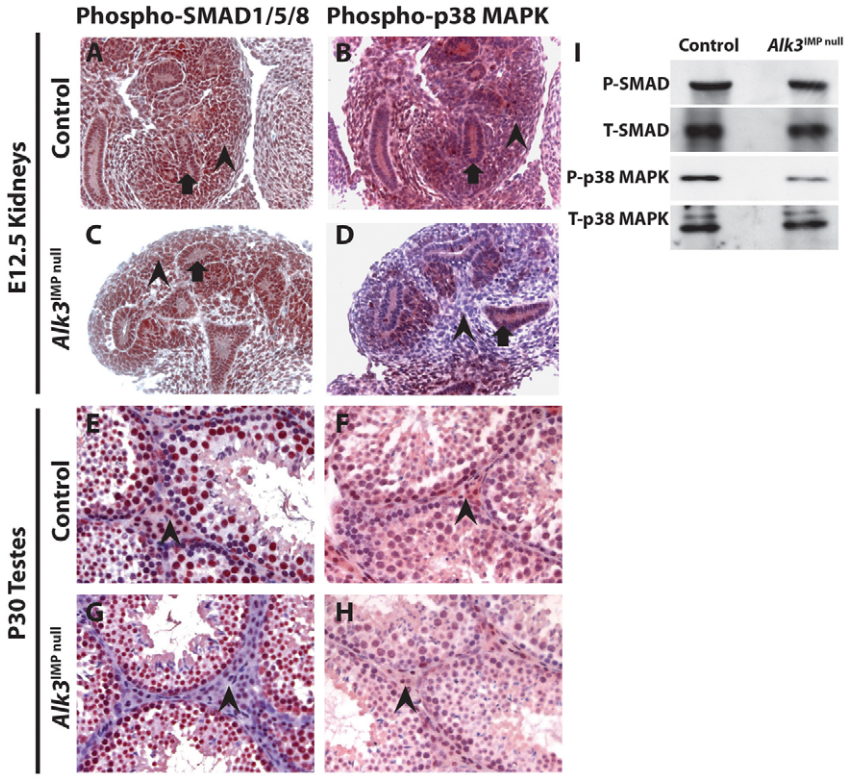

Fig. 6. Expression of BMP signaling effectors. (**A**) At E12.5, phospho-SMAD1/5/8 expression marked control ureteric cells (arrow) and the metanephric mesenchyme (arrowhead). (**C**) The phospho-SMAD1/5/8 renal expression domain was identical in *Alk3*$^{IMP\ null}$ mice. (**B**) At E12.5, phospho-p38 MAPK expression was observed in control ureteric bud cells (arrow) and the metanephric mesenchyme (arrowhead). (**D**) By contrast, whereas phospho-p38 MAPK was expressed in *Alk3*$^{IMP\ null}$ ureteric cells (arrow), expression was reduced in the uninduced metanephric mesenchyme (arrowhead). (**E**) At P30, phospho-SMAD1/5/8 is expressed in control testicular cells, including Leydig cells (arrowhead). (**G**) The expression of phospho-SMAD1/5/8 is reduced in Leydig cells in *Alk3*$^{IMP\ null}$ mice (arrowhead). (**F**,**H**) At P30, p38 MAPK was expressed in an identical manner in control (F) and *Alk3*$^{IMP\ null}$ (H) Leydig cells (arrowheads). (**I**) In E13.5 kidney protein lysate, phospho-p38 MAPK protein expression was reduced by 25% in *Alk3*$^{IMP\ null}$ kidneys. Phospho-SMAD1/5/8 protein levels were comparable between mutants and controls.

(Fig. 1I-J). We confirmed the reduction in mesonephric tubule number by using *lacZ* or PAX2 staining of whole-mount E11.5 urogenital ridges (Fig. 5A,B), in which all tubules can be examined in the same plane. In *Alk3*$^{IMP\ null}$ mice, mesonephric tubule number was significantly reduced (Fig. 5B, **P*<0.02). However, this reduction was not associated with increased apoptosis or decreased proliferation of mutant mesonephric tubule cells (see Fig. S5 in the supplementary material).

In the testis, peritubular myoid and interstitial Leydig cells are postulated to arise via cell migration from the mesonephros (Merchant-Larios and Moreno-Mendoza, 1998; Nishino et al., 2001). Analysis of E18.5 testis histological sections revealed fewer seminiferous tubules and a paucity of interstitial cells in *Alk3*$^{IMP\ null}$ mice (Fig. 5C,D), suggesting a mesonephros-derived cell defect. Peritubular myoid cells are required for seminiferous tubule integrity. Tubule integrity, assessed by location of SMA-marked peritubular myoid cells, appeared unaffected in mutants (see Fig. S5 in the supplementary material). Next, we assessed the Leydig cell population, which express *Rarb2*-Cre (Fig. 1E,F) and are marked by cytochrome P450 expression. Interestingly, at E18.5, fewer cytochrome P450-positive Leydig cells were present in *Alk3*$^{IMP\ null}$ males (Fig. 5H). Mutants also contained non-cytochrome P450-positive interstitial cells, indicative of defects in Leydig cell differentiation, which is dependent in part on testosterone levels. These results were confirmed using INSL3, an independent marker of Leydig cells (Fig. 5F,I). Analysis of INSL3-expressing cells revealed more loosely packed Leydig cells in the mutant interstitial compartment, a significantly lower number of Leydig cells compared with control (**P*=0.00), and a population of un-differentiated non-INSL3 expressing interstitial cells, consistent with our results using anti-cytochrome P450. During early postnatal life, androgen secretion from Leydig cells is required for initiation and maintenance of spermatogenesis, and sexual differentiation of the male brain for acquisition of copulatory and aggressive behaviors (Baker et al., 1996; Matsuda et al., 2008). Consistent with results in embryos, the number of Leydig cells was statistically decreased in P30 *Alk3*$^{IMP\ null}$ males (Fig. 5G,J,K).

Decreased Leydig cell number in *Alk3*$^{IMP\ null}$ mice suggested a possible decrease in testosterone production. Indeed, testosterone levels were significantly reduced in P30 mutant males (Fig. 5N). Mutant males also demonstrated physical and behavioral abnormalities consistent with reduced testosterone. Testosterone secretion stabilizes the nephric duct during seminal vesicle development (Hannema and Hughes, 2007). Although the seminal vesicle does not express *Rarb2*-Cre, (see Fig. S6 in the supplementary material), structural defects were present in *Alk3*$^{IMP\ null}$ males (Fig. 5O; see Fig. S6 in the supplementary material). The postnatal seminal vesicle contains a pseudo-stratified epithelial cell layer, arranged in intricate folds enclosing the seminal fluid (Fig. 5L). In *Alk3*$^{IMP\ null}$ males, the cell layer was thinner and demonstrated reduced branching morphogenesis (Fig. 5O). Testosterone is also required for copulatory behavior. Six-week old control and *Alk3*$^{IMP\ null}$ males were caged with naturally cycling 5-week-old females for 2 months. During this period, the mutant male did not sire offspring or demonstrate mating behavior, whereas control males fathered two litters of pups each. Finally, low testosterone is associated with decreased body size (Ingman and Robertson, 2007); postnatal *Alk3*$^{IMP\ null}$ males were on average 30% smaller than control (*n*=3). Together, these data demonstrate that *Alk3* deficiency decreases testosterone and adversely affects testosterone-dependent morphogenesis and behavior.

Alk3 is required for epididymis integrity

Portions of the intermediate mesoderm-derived nephric duct contribute to the epididymis (Joseph et al., 2009). *Rarb2*-Cre epididymis expression (Fig. 1F) allowed us to assess the requirement for ALK3 during this process. The epididymis is a highly coiled epithelial tube required for sperm maturation, and can

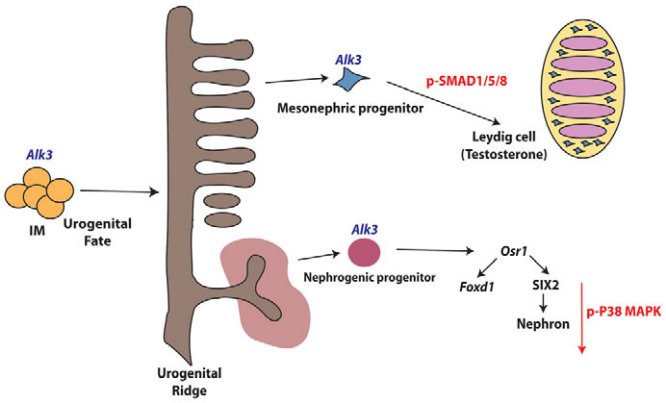

Fig. 7. *Alk3* signaling is required for intermediate mesoderm specification. In the intermediate mesoderm, ALK3 regulates nephrogenic progenitor cell number and the expression of renal progenitor genes (*Osr1*, SIX2). In the metanephric mesenchyme, ALK3 signals through the p38 MAPK pathway during nephrogenesis. ALK3 also regulates mesonephric tubule formation and the number of derivative Leydig cells. In the testis, ALK3 signals through the SMAD1/5/8 pathway during Leydig cell development.

be divided into three morphologically distinct domains: the caput, corpus and cauda. The finding of caput and cauda degeneration in *Bmp8a*$^{-/-}$ and compound *Bmp7*$^{+/-}$*; Bmp8a*$^{-/-}$ mice (Zhao et al., 2001) and of corpus degeneration in *Bmp4*$^{+/-}$ mice (Hu et al., 2004) demonstrated a requirement for BMP signaling in epididymis development. We found disorganization and vacuolation of corpus epithelial cells in *Alk3*$^{\text{IMP null}}$ animals (Fig. 5P), a phenotype consistent with *Bmp4*$^{+/-}$ mice. This data suggests that ALK3 is the receptor for BMP4, but not BMP7 or BMP8a, during epididymis morphogenesis.

Alk3$^{\text{IMP null}}$ mice demonstrated reduced activation of BMP intracellular signaling

BMPs signal via distinct canonical and non-canonical intracellular signaling pathways. Although previous work in mice with *Alk3* deficiency targeted to ureteric cells demonstrated that ALK3 signals via SMAD 1/5/8 (Hartwig et al., 2008), the intracellular effectors that function downstream of ALK3 in the metanephric mesenchyme and Leydig cells are undefined. We investigated ALK3-dependent signaling pathways by using antibodies directed against SMAD or MAPK BMP effectors. In contrast to the *Alk3*$^{\text{UB null}}$, expression of phospho-SMAD1/5/8 protein did not differ in kidneys isolated from E12.5 mutant and control mice (Fig. 6A,C). Rather, *Alk3*$^{\text{IMP null}}$ kidneys demonstrated reduced expression of phospho-p38 MAPK (Fig. 6B). In mutants, phospho-p38 MAPK expression was specifically reduced in the uninduced metanephric mesenchyme (Fig. 6D) – the location of nephrogenic progenitors. These results were confirmed by quantification of phospho-p38 MAPK protein, which demonstrated a 25% decrease in E13.5 *Alk3*$^{\text{IMP null}}$ kidney lysate (Fig. 6I). By contrast, expression of phospho-ERK1/2, another non-canonical BMP effector, was unchanged in mutants (see Fig. S7 in the supplementary material).

A parallel analysis in testis tissue revealed an opposite result. Here, phospho-SMAD1/5/8 was expressed in all cells in controls (Fig. 6E). However in *Alk3*$^{\text{IMP null}}$ mice, phospho-SMAD1/5/8 expression was decreased specifically in Leydig cells (Fig. 6G). In contrast to our findings in kidney tissue, phospho-p38 MAPK expression was unchanged in mutant versus control testis tissue (Fig. 6F,H). Thus, ALK3 signals in an organ-specific matter in intermediate mesoderm-derived cells.

DISCUSSION

The intermediate mesoderm gives rise to the permanent kidney and to components of the male genital system in mice. Previous studies have implicated BMP-ALK signaling in intermediate mesoderm gene expression (James and Schultheiss, 2005). However, the physiological functions of ALK-dependent signaling have been undefined. Here, we investigated these functions by targeting *Alk3* deficiency to intermediate mesoderm progenitor populations and their derivative structures using *Rarb2*-Cre and *Alk3*^{loxP} mice. Our results provide novel insights into nephrogenesis and testicular androgen production, and expand on a previous body of knowledge that had focused only on regulation of renal branching morphogenesis and of Mullerian duct regression, and germ cell development and migration (Jamin et al., 2002; Pellegrini et al., 2003; Hartwig et al., 2008; Dudley et al., 2010).

The renal progenitor population is reduced in *Alk3*$^{\text{IMP null}}$ mice

Extrinsic signals are required for commitment of the intermediate mesoderm to a renal lineage. Renal specification and formation of the first primitive kidney requires the development of the nephric duct, which can be induced to form by BMP4-soaked beads in the absence of the overlying surface ectoderm (Obara-Ishihara et al., 1999). However, the cell-autonomous requirement for BMP signaling during murine intermediate mesoderm specification had not been previously investigated. Our results indicate that *Alk3* controls metanephric blastema specification from the intermediate mesoderm. The smaller metanephric blastema consists of a reduced metanephric mesenchyme population in *Alk3*$^{\text{IMP null}}$ mice. Remarkably, the adrenal gland, which is partly derived from the intermediate mesoderm, was normal in mutants, supporting a specific effect of *Alk3* deficiency (see Fig. S1D in the supplementary material). Decreased expression of *Osr1* in *Alk3*$^{\text{IMP null}}$ mice suggests that *Alk3* functions upstream of *Osr1* to control the generation of *Foxd1*-positive stromal and SIX2-positive nephrogenic cell populations (Fig. 7). Reduction in the SIX2-positive nephrogenic progenitor population has been recognized in other cases of reduced nephron endowment in humans and mice (Weber et al., 2008; Fogelgren et al., 2009).

BMP signaling has previously been implicated in regulation of nephron number. Deletion of the pro-BMP molecule *Cv2* or podocyte-specific deletion of *Bmp7* both result in reduced nephron number (Kazama et al., 2008; Ikeya et al., 2010). However, our results are unique in that they provide direct insight into the functions of BMP signaling in nephrogenic progenitor cells. Our studies suggest that *Alk3* is not required for nephrogenesis after the stage at which the first phase of nephron progenitor development occurs. We found no evidence for a delay in nephrogenesis, as had been observed in cadherin 6 mutants (Mah et al., 2000). Nor was decreased nephrogenesis in *Alk3*$^{\text{IMP null}}$ mice associated with abnormal nephron differentiation, as is observed in mice deficient in *Wnt4*, *Lim1* or *Fgf8* expression (Grieshammer et al., 2005; Kobayashi et al., 2005). In contrast to other metanephric mesenchyme targeted models of renal hypoplasia, including *Myc*, *Mycn* and *Pax2* mutants, decreased nephrogenesis in *Alk3*$^{\text{IMP null}}$ mice could not attributed to reduced cell survival (Bates et al., 2000; Dziarmaga et al., 2003; Couillard and Trudel, 2009). Furthermore, the lack of effect of *Alk3* deficiency on cell

proliferation and apoptosis is distinct from that observed in *Bmp2*$^{+/-}$, *Smad4*$^{+/-}$ mice, which demonstrate reduced mesenchymal proliferation, and *Bmp7*$^{-/-}$ mice, which are characterized by metanephric mesenchyme cell apoptosis (Dudley and Robertson, 1997; Hartwig et al., 2005). Together, these observations suggest that ALK3 signals in the metanephric mesenchyme via molecular pathways that are distinct from those controlled by SMAD4 and BMP7.

Alk3 signaling regulates mesonephric derived testicular populations

Our results demonstrate a functional requirement for *Alk3* in intermediate mesoderm-derived testis cells. The murine testis is formed from genital swellings ventral to the mesonephros, which are populated by migrating primordial germ cells at E10.5 (Wilhelm and Koopman, 2006). BMP signaling regulates primordial germ cell number, proliferation and migration, yet no role had been defined in testicular somatic cells (Hu et al., 2004; Puglisi et al., 2004; Dudley et al., 2007). No germ cell defects were observed in *Alk3*$^{\text{IMP null}}$ mice, consistent with lack of expression of *Rarb2*-Cre in these cells. Indeed, abnormalities were observed only in cells derived from the Cre-expressing mesonephric progenitor cells.

The mesonephric origin of peritubular myoid cells is controversial (Nishino et al., 2001; Cool et al., 2008). Based on the mesonephric expression pattern of *Rarb2*-Cre, and the presence of flattened *lacZ*-expressing cells in the periphery of E15.5 seminiferous tubules (Fig. 1E), our data suggest that peritubular myoid cells are of mesonephric origin. However, the peritubular myoid cells do not require ALK3 signaling for differentiation, as SMA expression was normal in *Alk3*$^{\text{IMP null}}$ males. Defective peritubular myoid cell differentiation was observed in *Dhh*$^{-/-}$ males (Clark et al., 2000), and was associated the presence of germ cells in interstitial space, which was never noted in our model. ALK3 is required for Leydig cell development, explaining the paucity of interstitial cells noted in E18.5 mutant testes (Fig. 5D,H,I). The significant reduction in P30 Leydig cell number in *Alk3*$^{\text{IMP null}}$ males was further supported by reduced serum testosterone.

Low testosterone levels in *Alk3*$^{\text{IMP null}}$ males may have contributed to their inability to sire offspring. We postulate that low testosterone resulted in reduced copulatory behavior in *Alk3* mutants. Analysis of androgen receptor knockouts have shown that testosterone itself is required for differentiation of adult Leydig cells (Hardy et al., 1990; Murphy et al., 1994; Wang et al., 2009), which are marked by the expression of steroidogenic enzymes such as cytochrome P450. Indeed, we noted non-expressing cells in E18.5 mutant tissue (Fig. 5H), which may have further contributed to reduced testosterone production. Low testosterone is also associated with seminal vesicle developmental defects (Hannema and Hughes, 2007), which were present in *Alk3*$^{\text{IMP null}}$ males. The seminal fluid is required for sperm nourishment and integrity, so abnormal seminal vesicle development may contribute to *Alk3*$^{\text{IMP null}}$ male infertility. Low testosterone is associated with 20-30% of cases of human male infertility (Dohle et al., 2003). Our results may indicate a role for BMP signaling in the etiology of male sexual dysfunction.

We also demonstrated that ALK3 is required for epididymis integrity in a ligand-specific manner. BMP4 is expressed through the entire epididymis epithelium (Hu et al., 2004), as is *Rarb2*-Cre. However, BMP7 and BMP8a/b expression are only observed in the caput and cauda (Zhao et al., 2001), and therefore do not control corpus epididymis development. The epithelial vacuolation observed in the *Alk3*$^{\text{IMP null}}$ corpus epididymis (Fig. 5P) is comparable with abnormalities noted in *Bmp4*$^{+/-}$ males (Hu et al., 2004). Based on our data, we postulate that during epididymis morphogenesis, BMP4 signaling requires ALK3, whereas BMP7 and/or BMP8a/b signaling through other BMP receptors compensates for *Alk3* deletion during cauda and caput formation. ALK6 is ubiquitously expressed in the epididymis and the expression pattern of ALK2 is unknown (Hu et al., 2004). Epididymis defects affect sperm motility and integrity, and may contribute to the inability of *Alk3*$^{\text{IMP null}}$ males to sire offspring.

Alk3 utilizes different downstream signaling mechanisms in a tissue-specific manner

During renal development, ALK3 signals via SMAD proteins in ureteric cells (Hu et al., 2003; Hartwig et al., 2008). Our data demonstrated that ALK3 signals via MAPKs in the metanephric mesenchyme (Fig. 7). These results are consistent with previous findings. Analysis of a SMAD-dependent BMP signaling reporter mouse found no reporter activity in developing nephrons or progenitor cells (Blank et al., 2008). Treatment of ex vivo kidney explants with p38MAPK inhibitors attenuates nephrogenesis (Hida et al., 2002). Renal hypoplasia in mice with *Bmp7* deficiency targeted to podocytes is also associated with reduced p38MAPK activity and normal SMAD expression (Kazama et al., 2008). By contrast, the pro-BMP factor *Cv2* mediates metanephric mesenchyme cell adhesion and nephrogenesis through SMAD signaling (Ikeya et al., 2010). However, *Cv2* appears to act downstream of BMP7, which is thought to signal via ALK2.

In contrast to the metanephric mesenchyme, our results show that ALK3 regulates SMAD, but not p38MAPK signaling in the testis (Fig. 7). Previous studies show that the BMP-dependent SMADS, SMAD1 and SMAD5, are required for primordial germ cell specification (Arnold et al., 2006). We demonstrated that phospho-SMAD1/5/8 is ubiquitously activated in the developing testis, pointing to an additional requirement for SMAD signaling in somatic testicular cells. Consistent with this requirement, the mesonephric derived Leydig cells demonstrated reduced SMAD activity. These data demonstrate a requirement for BMP-induced SMAD activity in somatic androgen-producing cells during testis development.

In summary, we have demonstrated that *Alk3* is required for specification of urogenital development from the intermediate mesoderm (Fig. 7). During renal development, *Alk3* regulates formation of the metanephric blastema and controls the number of *Osr1*- and SIX2-expressing nephrogenic progenitor cells. *Alk3* also controls nephrogenesis that uses p38 MAPK signaling. Similarly, *Alk3* controls mesonephric tubule and derivative Leydig cell number through SMAD1/5/8 signaling. Different BMP signaling pathways are used in the different progenitor compartments. These results not only delineate a role for BMP signaling during intermediate mesoderm specification, but also in urogenital disease.

Acknowledgements

This work was supported by an operating grant from the Canadian Institutes of Health Research (to N.D.R.) and a Canada Research Chair (to N.D.R.). The authors also thank Dr Carlton Bates and Dr Sunder Sims-Lucas for facilitating the acquisition of the INSL3 expression data.

Competing interests statement

The authors declare no competing financial interests.

Supplementary material

Supplementary material for this article is available at
http://dev.biologists.org/lookup/suppl/doi:10.1242/dev.059030/-/DC1

References

Arnold, S. J., Maretto, S., Islam, A., Bikoff, E. K. and Robertson, E. J. (2006). Dose-dependent Smad1, Smad5 and Smad8 signaling in the early mouse embryo. *Dev. Biol.* **296**, 104-118.

Baker, J., Hardy, M. P., Zhou, J., Bondy, C., Lupu, F., Bellve, A. R. and Efstratiadis, A. (1996). Effects of an Igf1 gene null mutation on mouse reproduction. *Mol. Endocrinol.* **10**, 903-918.

Bates, C. M., Kharzai, S., Erwin, T., Rossant, J. and Parada, L. F. (2000). Role of N-myc in the developing mouse kidney. *Dev. Biol.* **222**, 317-325.

Blank, U., Seto, M. L., Adams, D. C., Wojchowski, D. M., Karolak, M. J. and Oxburgh, L. (2008). An in vivo reporter of BMP signaling in organogenesis reveals targets in the developing kidney. *BMC Dev. Biol.* **8**, 86.

Buehr, M., Gu, S. and McLaren, A. (1993). Mesonephric contribution to testis differentiation in the fetal mouse. *Development* **117**, 273-281.

Cain, J. E., Islam, E., Haxho, F., Chen, L., Bridgewater, D., Nieuwenhuis, E., Hui, C. C. and Rosenblum, N. D. (2009). GLI3 repressor controls nephron number via regulation of Wnt11 and Ret in ureteric tip cells. *PLoS ONE* **4**, e7313.

Cain, J. E., Di Giovanni, V., Smeeton, J. and Rosenblum, N. D. (2010). Genetics of renal hypoplasia: insights into the mechanisms controlling nephron endowment. *Pediatr. Res.* **68**, 91-98.

Carroll, T. J., Park, J. S., Hayashi, S., Majumdar, A. and McMahon, A. P. (2005). Wnt9b plays a central role in the regulation of mesenchymal to epithelial transitions underlying organogenesis of the mammalian urogenital system. *Dev. Cell* **9**, 283-292.

Clark, A. M., Garland, K. K. and Russell, L. D. (2000). Desert hedgehog (Dhh) gene is required in the mouse testis for formation of adult-type Leydig cells and normal development of peritubular cells and seminiferous tubules. *Biol. Reprod.* **63**, 1825-1838.

Combes, A. N., Wilhelm, D., Davidson, T., Dejana, E., Harley, V., Sinclair, A. and Koopman, P. (2009). Endothelial cell migration directs testis cord formation. *Dev. Biol.* **326**, 112-120.

Cool, J., Carmona, F. D., Szucsik, J. C. and Capel, B. (2008). Peritubular myoid cells are not the migrating population required for testis cord formation in the XY gonad. *Sex. Dev.* **2**, 128-133.

Couillard, M. and Trudel, M. (2009). C-myc as a modulator of renal stem/progenitor cell population. *Dev. Dyn.* **238**, 405-414.

Dewulf, N., Verschueren, K., Lonnoy, O., Moren, A., Grimsby, S., Vande Spiegle, K., Miyazono, K., Huylebroeck, D. and Ten Dijke, P. (1995). Distinct spatial and temporal expression patterns of two type I receptors for bone morphogenetic proteins during mouse embryogenesis. *Endocrinology* **136**, 2652-2663.

Dick, A., Hild, M., Bauer, H., Imai, Y., Maifeld, H., Schier, A. F., Talbot, W. S., Bouwmeester, T. and Hammerschmidt, M. (2000). Essential role of Bmp7 (snailhouse) and its prodomain in dorsoventral patterning of the zebrafish embryo. *Development* **127**, 343-354.

Dohle, G. R., Smit, M. and Weber, R. F. (2003). Androgens and male fertility. *World J. Urol.* **21**, 341-345.

Dressler, G. R. (2009). Advances in early kidney specification, development and patterning. *Development* **136**, 3863-3874.

Dudley, A. T. and Robertson, E. J. (1997). Overlapping expression domains of bone morphogenetic protein family members potentially account for limited tissue defects in BMP7 deficient embryos. *Dev. Dyn.* **208**, 349-362.

Dudley, B., Palumbo, C., Nalepka, J. and Molyneaux, K. (2010). BMP signaling controls formation of a primordial germ cell niche within the early genital ridges. *Dev. Biol.* **343**, 84-93.

Dudley, B. M., Runyan, C., Takeuchi, Y., Schaible, K. and Molyneaux, K. (2007). BMP signaling regulates PGC numbers and motility in organ culture. *Mech. Dev.* **124**, 68-77.

Dyche, W. J. (1979). A comparative study of the differentiation and involution of the Mullerian duct and Wolffian duct in the male and female fetal mouse. *J. Morphol.* **162**, 175-209.

Dziarmaga, A., Clark, P., Stayner, C., Julien, J. P., Torban, E., Goodyer, P. and Eccles, M. (2003). Ureteric bud apoptosis and renal hypoplasia in transgenic PAX2-Bax fetal mice mimics the renal-coloboma syndrome. *J. Am. Soc. Nephrol.* **14**, 2767-2774.

Fogelgren, B., Yang, S., Sharp, I. C., Huckstep, O. J., Ma, W., Somponpun, S. J., Carlson, E. C., Uyehara, C. F. and Lozanoff, S. (2009). Deficiency in Six2 during prenatal development is associated with reduced nephron number, chronic renal failure, and hypertension in Br/+ adult mice. *Am. J. Physiol. Renal Physiol.* **296**, F1166-F1178.

Grieshammer, U., Cebrian, C., Ilagan, R., Meyers, E., Herzlinger, D. and Martin, G. R. (2005). FGF8 is required for cell survival at distinct stages of nephrogenesis and for regulation of gene expression in nascent nephrons. *Development* **132**, 3847-3857.

Grobstein, C. (1956). Trans-filter induction of tubules in mouse metanephrogenic mesenchyme. *Exp. Cell Res.* **10**, 424-440.

Hannema, S. E. and Hughes, I. A. (2007). Regulation of Wolffian duct development. *Horm. Res.* **67**, 142-151.

Hardy, M. P., Kelce, W. R., Klinefelter, G. R. and Ewing, L. L. (1990). Differentiation of Leydig cell precursors in vitro: a role for androgen. *Endocrinology* **127**, 488-490.

Hartwig, S., Hu, M. C., Cella, C., Piscione, T., Filmus, J. and Rosenblum, N. D. (2005). Glypican-3 modulates inhibitory Bmp2-Smad signaling to control renal development in vivo. *Mech. Dev.* **122**, 928-938.

Hartwig, S., Bridgewater, D., Di Giovanni, V., Cain, J., Mishina, Y. and Rosenblum, N. D. (2008). BMP receptor ALK3 controls collecting system development. *J. Am. Soc. Nephrol.* **19**, 117-124.

Hebert, J. M., Mishina, Y. and McConnell, S. K. (2002). BMP signaling is required locally to pattern the dorsal telencephalic midline. *Neuron* **35**, 1029-1041.

Hida, M., Omori, S. and Awazu, M. (2002). ERK and p38 MAP kinase are required for rat renal development. *Kidney Int.* **61**, 1252-1262.

Hu, G. X., Lin, H., Chen, G. R., Chen, B. B., Lian, Q. Q., Hardy, D. O., Zirkin, B. R. and Ge, R. S. (2010). Deletion of the IGF-I gene: suppressive effects on adult leydig cell development. *J. Androl.* **31**, 379-387.

Hu, J., Chen, Y. X., Wang, D., Qi, X., Li, T. G., Hao, J., Mishina, Y., Garbers, D. L. and Zhao, G. Q. (2004). Developmental expression and function of Bmp4 in spermatogenesis and in maintaining epididymal integrity. *Dev. Biol.* **276**, 158-171.

Hu, M. C., Piscione, T. D. and Rosenblum, N. D. (2003). Elevated SMAD1/beta-catenin molecular complexes and renal medullary cystic dysplasia in ALK3 transgenic mice. *Development* **130**, 2753-2766.

Ikeya, M., Fukushima, K., Kawada, M., Onishi, S., Furuta, Y., Yonemura, S., Kitamura, T., Nosaka, T. and Sasai, Y. (2010). Cv2, functioning as a pro-BMP factor via twisted gastrulation, is required for early development of nephron precursors. *Dev. Biol.* **337**, 405-414.

Ingman, W. V. and Robertson, S. A. (2007). Transforming growth factor-beta1 null mutation causes infertility in male mice associated with testosterone deficiency and sexual dysfunction. *Endocrinology* **148**, 4032-4043.

James, R. G. and Schultheiss, T. M. (2005). Bmp signaling promotes intermediate mesoderm gene expression in a dose-dependent, cell-autonomous and translation-dependent manner. *Dev. Biol.* **288**, 113-125.

Jamin, S. P., Arango, N. A., Mishina, Y., Hanks, M. C. and Behringer, R. R. (2002). Requirement of Bmpr1a for Mullerian duct regression during male sexual development. *Nat. Genet.* **32**, 408-410.

Joseph, A., Yao, H. and Hinton, B. T. (2009). Development and morphogenesis of the Wolffian/epididymal duct, more twists and turns. *Dev. Biol.* **325**, 6-14.

Karl, J. and Capel, B. (1998). Sertoli cells of the mouse testis originate from the coelomic epithelium. *Dev. Biol.* **203**, 323-333.

Kazama, I., Mahoney, Z., Miner, J. H., Graf, D., Economides, A. N. and Kreidberg, J. A. (2008). Podocyte-derived BMP7 is critical for nephron development. *J. Am. Soc. Nephrol.* **19**, 2181-2191.

Kishimoto, Y., Lee, K. H., Zon, L., Hammerschmidt, M. and Schulte-Merker, S. (1997). The molecular nature of zebrafish swirl: BMP2 function is essential during early dorsoventral patterning. *Development* **124**, 4457-4466.

Klein, G., Langegger, M., Goridis, C. and Ekblom, P. (1988). Neural cell adhesion molecules during embryonic induction and development of the kidney. *Development* **102**, 749-761.

Kobayashi, A., Kwan, K. M., Carroll, T. J., McMahon, A. P., Mendelsohn, C. L. and Behringer, R. R. (2005). Distinct and sequential tissue-specific activities of the LIM-class homeobox gene Lim1 for tubular morphogenesis during kidney development. *Development* **132**, 2809-2823.

Kobayashi, A., Valerius, M. T., Mugford, J. W., Carroll, T. J., Self, M., Oliver, G. and McMahon, A. P. (2008). Six2 defines and regulates a multipotent self-renewing nephron progenitor population throughout mammalian kidney development. *Cell Stem Cell* **3**, 169-181.

Kuure, S., Vuolteenaho, R. and Vainio, S. (2000). Kidney morphogenesis: cellular and molecular regulation. *Mech. Dev.* **92**, 31-45.

Lambert, J. F., Benoit, B. O., Colvin, G. A., Carlson, J., Delville, Y. and Quesenberry, P. J. (2000). Quick sex determination of mouse fetuses. *J. Neurosci. Methods* **95**, 127-132.

Lawson, K. A. and Hage, W. J. (1994). Clonal analysis of the origin of primordial germ cells in the mouse. *Ciba Found. Symp.* **182**, 68-84; discussion 84-91.

Lawson, K. A., Dunn, N. R., Roelen, B. A., Zeinstra, L. M., Davis, A. M., Wright, C. V., Korving, J. P. and Hogan, B. L. (1999). Bmp4 is required for the generation of primordial germ cells in the mouse embryo. *Genes Dev.* **13**, 424-436.

Mah, S. P., Saueressig, H., Goulding, M., Kintner, C. and Dressler, G. R. (2000). Kidney development in cadherin-6 mutants: delayed mesenchyme-to-epithelial conversion and loss of nephrons. *Dev. Biol.* **223**, 38-53.

Matsuda, K., Sakamoto, H. and Kawata, M. (2008). Androgen action in the brain and spinal cord for the regulation of male sexual behaviors. *Curr. Opin. Pharmacol.* **8**, 747-751.

Merchant-Larios, H. and Moreno-Mendoza, N. (1998). Mesonephric stromal cells differentiate into Leydig cells in the mouse fetal testis. *Exp. Cell Res.* **244**, 230-238.

Merchant-Larios, H., Moreno-Mendoza, N. and Buehr, M. (1993). The role of the mesonephros in cell differentiation and morphogenesis of the mouse fetal testis. *Int. J. Dev. Biol.* **37**, 407-415.
Mishina, Y., Suzuki, A., Ueno, N. and Behringer, R. R. (1995). Bmpr encodes a type I bone morphogenetic protein receptor that is essential for gastrulation during mouse embryogenesis. *Genes Dev.* **9**, 3027-3037.
Mishina, Y., Hanks, M. C., Miura, S., Tallquist, M. D. and Behringer, R. R. (2002). Generation of Bmpr/Alk3 conditional knockout mice. *Genesis* **32**, 69-72.
Mugford, J. W., Sipila, P., McMahon, J. A. and McMahon, A. P. (2008). Osr1 expression demarcates a multi-potent population of intermediate mesoderm that undergoes progressive restriction to an Osr1-dependent nephron progenitor compartment within the mammalian kidney. *Dev. Biol.* **324**, 88-98.
Murphy, L., Jeffcoate, I. A. and O'Shaughnessy, P. J. (1994). Abnormal Leydig cell development at puberty in the androgen-resistant Tfm mouse. *Endocrinology* **135**, 1372-1377.
Narlis, M., Grote, D., Gaitan, Y., Boualia, S. K. and Bouchard, M. (2007). Pax2 and pax8 regulate branching morphogenesis and nephron differentiation in the developing kidney. *J. Am. Soc. Nephrol.* **18**, 1121-1129.
Nishino, K., Yamanouchi, K., Naito, K. and Tojo, H. (2001). Characterization of mesonephric cells that migrate into the XY gonad during testis differentiation. *Exp. Cell Res.* **267**, 225-232.
Nohe, A., Keating, E., Knaus, P. and Petersen, N. O. (2004). Signal transduction of bone morphogenetic protein receptors. *Cell. Signal.* **16**, 291-299.
Obara-Ishihara, T., Kuhlman, J., Niswander, L. and Herzlinger, D. (1999). The surface ectoderm is essential for nephric duct formation in intermediate mesoderm. *Development* **126**, 1103-1108.
Pellegrini, M., Grimaldi, P., Rossi, P., Geremia, R. and Dolci, S. (2003). Developmental expression of BMP4/ALK3/SMAD5 signaling pathway in the mouse testis: a potential role of BMP4 in spermatogonia differentiation. *J. Cell Sci.* **116**, 3363-3372.
Preger-Ben Noon, E., Barak, H., Guttmann-Raviv, N. and Reshef, R. (2009). Interplay between activin and Hox genes determines the formation of the kidney morphogenetic field. *Development* **136**, 1995-2004.
Puglisi, R., Montanari, M., Chiarella, P., Stefanini, M. and Boitani, C. (2004). Regulatory role of BMP2 and BMP7 in spermatogonia and Sertoli cell proliferation in the immature mouse. *Eur. J. Endocrinol.* **151**, 511-520.
Saxen, L. (1987). *Organogenesis of the Kidney*. Cambridge: Press Syndicate of the University of Cambridge.
Saxen, L. and Sariola, H. (1987). Early organogenesis of the kidney. *Pediatr. Nephrol.* **1**, 385-392.
Saxen, L., Sariola, H. and Lehtonen, E. (1986). Sequential cell and tissue interactions governing organogenesis of the kidney. *Anat. Embryol. (Berl.)* **175**, 1-6.
Schedl, A. (2007). Renal abnormalities and their developmental origin. *Nat. Rev. Genet.* **8**, 791-802.
Self, M., Lagutin, O. V., Bowling, B., Hendrix, J., Cai, Y., Dressler, G. R. and Oliver, G. (2006). Six2 is required for suppression of nephrogenesis and progenitor renewal in the developing kidney. *EMBO J.* **25**, 5214-5228.
Soriano, P. (1999). Generalized lacZ expression with the ROSA26 Cre reporter strain. *Nat. Genet.* **21**, 70-71.
Stark, K., Vainio, S., Vassileva, G. and McMahon, A. P. (1994). Epithelial transformation of metanephric mesenchyme in the developing kidney regulated by Wnt-4. *Nature* **372**, 679-683.
ten Dijke, P., Yamashita, H., Sampath, T. K., Reddi, A. H., Estevez, M., Riddle, D. L., Ichijo, H., Heldin, C. H. and Miyazono, K. (1994). Identification of type I receptors for osteogenic protein-1 and bone morphogenetic protein-4. *J. Biol. Chem.* **269**, 16985-16988.
Vainio, S. and Lin, Y. (2002). Coordinating early kidney development: lessons from gene targeting. *Nat. Rev. Genet.* **3**, 533-543.
Wang, R. S., Yeh, S., Tzeng, C. R. and Chang, C. (2009). Androgen receptor roles in spermatogenesis and fertility: lessons from testicular cell-specific androgen receptor knockout mice. *Endocr. Rev.* **30**, 119-132.
Weber, S., Taylor, J. C., Winyard, P., Baker, K. F., Sullivan-Brown, J., Schild, R., Knuppel, T., Zurowska, A. M., Caldas-Alfonso, A., Litwin, M. et al. (2008). SIX2 and BMP4 mutations associate with anomalous kidney development. *J. Am. Soc. Nephrol.* **19**, 891-903.
Wilhelm, D. and Koopman, P. (2006). The makings of maleness: towards an integrated view of male sexual development. *Nat. Rev. Genet.* **7**, 620-631.
Winnier, G., Blessing, M., Labosky, P. A. and Hogan, B. L. (1995). Bone morphogenetic protein-4 is required for mesoderm formation and patterning in the mouse. *Genes Dev.* **9**, 2105-2116.
Ying, Y. and Zhao, G. Q. (2001). Cooperation of endoderm-derived BMP2 and extraembryonic ectoderm-derived BMP4 in primordial germ cell generation in the mouse. *Dev. Biol.* **232**, 484-492.
Zhang, H. and Bradley, A. (1996). Mice deficient for BMP2 are nonviable and have defects in amnion/chorion and cardiac development. *Development* **122**, 2977-2986.
Zhao, G. Q., Chen, Y. X., Liu, X. M., Xu, Z. and Qi, X. (2001). Mutation in Bmp7 exacerbates the phenotype of Bmp8a mutants in spermatogenesis and epididymis. *Dev. Biol.* **240**, 212-222.